Transition Metal Derivatives of a Chelating Nitronyl Nitroxide Ligand. Nickel(II) and Manganese(II) Complexes

Dominique Luneau,† Gérard Risoan,† Paul Rey,*,† André Grand,† Andrea Caneschi,‡ Dante Gatteschi,‡ and Jean Laugier†

Laboratoire de Chimie de coordination (URA CNRS 1194), Service d'Etude des Systèmes et Architectures Moléculaires, and Service de Physique des Matériaux et Microstructures, Département de Recherche Fondamentale, Centre d'Etudes Nucléaires, 38041 Grenoble, France, and Department of Chemistry, University of Florence, Florence, Italy

Received February 2, 1993•

Complexes of the nitroxide ligand 2-(2-pyridyl)-4,4,5,5-tetramethyl-4,5-dihydro-1*H*-imidazolyl-1-oxy 3-oxide (NIT2-Py) with $NiCl_2$ (**1**, $C_{26}H_{36}Cl_6N_6NiO_4$) and $MnCl_2$ (**2**, $C_{26}H_{36}Cl_6MnN_6O_4$) have been structurally and magnetically characterized. Both complexes are centrosymmetric three-spin systems in which the nitroxyl group is coordinated to the metal ion. Metal–nitroxide interactions of -110 cm^{-1} for **1** and -80 cm^{-1} for **2** ($H = -2JS_iS_j$) are observed. These coupling constants are weaker than usually observed in previously reported examples (<-200 cm^{-1} for Ni and -150, -200 cm^{-1} for Mn). This result was rationalized by considering a reduced overlap of the magnetic orbitals due to a peculiar geometric arrangement in the chelate. Comparison to literature reported species is obtained from the homologous hexafluoroacetylacetonates, **3** ($C_{22}H_{18}F_{12}N_3NiO_6$) and **4** ($C_{22}H_{18}F_{12}MnN_3O_6$), which exhibit similar structural and magnetic properties. Coordination of the nitroxyl group in these derivatives illustrates the use of the chelate effect for designing exchange-coupled nitroxide derivatives of poor electrophilic metal centers. Relevant structural parameters are as follows: **1**, monoclinic, $P2_1/c$, $a = 8.890(2)$ Å, $b = 13.957(2)$ Å, $c = 13.802(2)$ Å, $\beta = 103.06(2)°$, $Z = 2$; **2**, monoclinic, $P2_1/c$, $a = 9.018(2)$ Å, $b = 13.815(3)$ Å, $c = 14.095(2)$ Å, $\beta = 102.90(2)°$, $Z = 2$; **3**, monoclinic, $P2_1/c$, $a = 11.866(3)$ Å, $b = 15.173(3)$ Å, $c = 17.282(3)$ Å, $\beta = 95.66(1)°$, $Z = 4$; **4**, monoclinic, $P2_1/c$, $a = 10.453(2)$ Å, $b = 16.518(3)$ Å, $c = 16.697(4)$ Å, $\beta = 94.08(1)°$, $Z = 4$.

The predominant magnetic features of metal–nitroxide complexes are determined by the donor properties of the nitroxyl group and the coordination geometry of the resulting complex.[1,2] Since nitroxides are weak Lewis bases,[3] they only bind to acid metal centers such as hexafluoroacetylacetonates[4] and a few metal halides (Cu(II),[5,6] Co(II)[7]). The binding geometry of the nitroxides to these metal precursors is highly dependent on both electronic and steric factors.[2] It is believed that the overlap of the magnetic orbitals and the partial pairing of the unpaired electrons stabilize the adduct explaining that most metal–nitroxide interactions are antiferromagnetic.[1] However, in the solid state, crystal packing interactions may be more stabilizing than the overlap of the magnetic orbitals leading to binding geometries responsible for weak ferromagnetic interactions.[8-12] These considerations must also include the characteristics of the chemical structure of the nitroxide ligand, which may favor unforseeable structures and magnetic behaviors.[13]

Hence, metal–nitroxide adducts are generally antiferromagnetically coupled species where the presence of the bulky hexafluoroacetylacetonato groups around the metal ion is a strong hindrance to obtaining bulk magnetic properties. However, using nitronyl nitroxides, chainlike species exhibiting spontaneous magnetization at low temperature were recently reported.[14,15] In these compounds, the intrachain interaction is large ($-J$, > 200 cm^{-1}) while the interchain coupling is weak, so that the critical temperatures are generally lower than 10 K. In order to design compounds exhibiting higher Curie temperatures, we are currently investigating the coordination chemistry of nitroxide ligands possessing nucleophilic properties and thus allowing the synthesis of metal derivatives using less hindered and less acidic metal centers.

In his pioneering work, Kreilick reported that some metal adducts of the pyridyl-substituted nitronyl nitroxides[16] were stable even in solution.[17,18] We characterized several complexes of the 4-pyridyl-substituted nitronyl nitroxide with first-row transition metal ions in which it was found that large exchange interactions were mediated by the pyridyl nitrogen atom.[19,20] Moreover,

† CEN.
‡ University of Florence.
• Abstract published in *Advance ACS Abstracts*, October 15, 1993.

(1) Caneschi, A.; Gatteschi, D.; Rey, P. *Prog. Inorg. Chem.* **1991**, *39*, 331–429 and references therein.
(2) Rey, P.; Laugier, J.; Caneschi, A.; Gatteschi, D. *Mol. Cryst. Liq. Cryst.* **1989**, *176*, 337–346.
(3) (a) Lim, Y. Y.; Drago, R. S. *J. Am. Chem. Soc.* **1971**, *93*, 891–894. (b) Lim, Y. Y.; Drago, R. S. *Inorg. Chem.* **1972**, *11*, 1334–1338. (c) Richman, R. M.; Kuechler, T. C.; Drago, R. S. *J. Am. Chem. Soc.* **1977**, *99*, 1055–1058. (d) Drago, R. S.; Kuechler, T. C.; Kroeger, M. *Inorg. Chem.* **1979**, *18*, 2337–2342.
(4) Zelonka, R. A.; Baird, M. C. *J. Am. Chem. Soc.* **1971**, *93*, 6066–6070.
(5) Jahr, D.; Rebhan, K. H.; Schwarzhans, K. E.; Wiedemann, J. *Z. Naturforsch.* **1973**, *28B*, 55–62.
(6) Laugier, J.; Rey, P.; Benelli, C.; Gatteschi, D.; Zanchini, C. *J. Am. Chem. Soc.* **1986**, *108*, 6931–6937.
(7) (a) Beck, W.; Schmidtner, K.; Keller, H. J. *Chem. Ber.* **1967**, *100*, 503–511. (b) Brown, D. G.; Maier, T.; Drago, R. S. *Inorg. Chem.* **1971**, *10*, 2804–2806. (c) Benelli, C.; Gatteschi, D.; Zanchini, C. *Inorg. Chem.* **1984**, *23*, 798–800.
(8) Grand, A.; Rey, P.; Subra, R. *Inorg. Chem.* **1983**, *22*, 391–394.
(9) Anderson, O. P.; Kuechler, T. C. *Inorg. Chem.* **1980**, *19*, 1417–1422.
(10) Caneschi, A.; Gatteschi, D.; Laugier, J.; Rey, P. *J. Am. Chem. Soc.* **1987**, *109*, 2191–2192.
(11) Caneschi, A.; Gatteschi, D.; Grand, A.; Laugier, J.; Pardi, L.; Rey, P. *Inorg. Chem.* **1988**, *27*, 1031–1035.
(12) Ovcharenko, V. I.; Ikorskii, V. N.; Podberezskaya, N. V.; Pervukhina, N. V.; Larionov, S. V. *Zh. Neorg. Khim.* **1987**, *32*, 1403–1406.
(13) Caneschi, A.; Gatteschi, D.; Laugier, J.; Rey, P.; Sessoli, R.; Zanchini, C. *J. Am. Chem. Soc.* **1988**, *110*, 2795–2799.
(14) Caneschi, A.; Gatteschi, D.; Renard, J.-P.; Rey, P.; Sessoli, R. *Inorg. Chem.* **1989**, *28*, 1976–1980.
(15) Caneshi, A.; Gatteschi, D.; Renard, J.-P.; Rey, P.; Sessoli, R. *Inorg. Chem.* **1989**, *28*, 2940–2944.
(16) Ullman, E. F.; Osiecki, J. H.; Boocock, D. G. B.; Darcy, R. *J. Am. Chem. Soc.* **1972**, *94*, 7049–7059.
(17) Richardson, P. F.; Kreilick, R. W. *J. Am. Chem. Soc.* **1977**, *99*, 8183–8187.
(18) Richardson, P. F.; Kreilick, R. M. *J. Phys. Chem.* **1978**, *82*, 1149–1151.
(19) Caneschi, A.; Ferraro, F.; Gatteschi, D.; Rey, P.; Sessoli, R. *Inorg. Chem.* **1990**, *29*, 1756–1760.
(20) Caneschi, A.; Ferraro, F.; Gatteschi, D.; Rey, P.; Sessoli, R. *Inorg. Chem.* **1990**, *29*, 4217–4223.

0020-1669/93/1332-5616$04.00/0

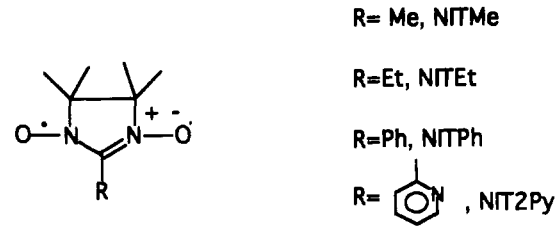

Figure 1. Chemical structure of the nitroxide ligands.

unusual magnetic behaviors such as weak ferromagnetic Mn(II)–nitroxide interactions were observed. Unfortunately, in these adducts, the NO groups of the radical are not coordinated even when the metal center is a strong Lewis acid.

The 2-pyridyl-substituted nitronyl nitroxide ligand (Figure 1) is especially attractive because the position of the pyridyl imino donor atom is such that it could enforce the coordination of the NO group by the chelate effect. It is expected, therefore, that coordination will occur with poor electrophilic metal centers; in addition, the formation of a ring structure comprising the two paramagnetic centers will predetermine the orientation of the magnetic orbitals and the magnetic behavior of the complex.

We describe here the structural characterization and the magnetic properties of the nickel(II) and manganese(II) chloride derivatives of 2-(2-pyridyl)-4,4,5,5-tetramethyl-4,5-dihydro-1*H*-imidazolyl-1-oxy 3-oxide (NIT2-Py). The homologous hexafluoroacetylacetonate complexes have also been investigated for comparison with previously reported nonchelated species. The chloride adducts illustrate the coordination of this free radical to weak electrophilic metal centers.

Experimental Section

Syntheses. 2-(2-Pyridyl)-4,4,5,5-tetramethyl-4,5-dihydro-1*H*-imidazolyl-1-oxy 3-oxide, NIT2-Py (Figure 1), nickel(II) and magnanese(II) bis(hexafluoroacetylacetonates), $Ni(hfac)_2$ and $Mn(hfac)_2$, were obtained by following previously reported procedures.[17,21]

(a) Metal Chloride Adducts. Bis(2-(2-pyridyl)-4,4,5,5-tetramethyl-4,5-dihydro-1*H*-imidazolyl-1-oxy 3-oxide)nickel(II) dichloride bis(methylene chloride) solvate, $NiCl_2(NIT2\text{-}Py)_2{\cdot}2CH_2Cl_2$ (**1**), and bis(2-(2-pyridyl)-4,4,5,5-tetramethyl-4,5-dihydro-1*H*-imidazolyl-1-oxy 3-oxide)manganese(II) dichloride bis(methylene chloride) solvate, $MnCl_2(NIT2\text{-}Py)_2{\cdot}2CH_2Cl_2$ (**2**), were obtained using the same procedure. A solution of 160 mg (0.68 mmol) of NIT2-Py in 5 mL of methylene chloride was poured into a 10 mm diameter tube. On the top was carefully added 1 mL of pure ethanol and then a solution of $^1/_2$ equiv of the appropriate metal chloride. The two solutions were allowed to diffuse in the dark at 6 °C. After 7 days, the precipitates were filtered off. They analyzed satisfactorily for **1** and **2**. $NiCl_2(NIT2\text{-}Py)_2{\cdot}2CH_2Cl_2$ (**1**): yield 45%; mp >300 °C. Anal. Calcd for $C_{26}H_{36}N_6O_4Cl_6Ni$: C, 40.64; H, 4.73; N, 10.95; O, 8.34; Cl, 27.71; Ni, 7.64. Found: C, 41.05; H, 5.01; N, 10.83; Cl, 27.57; Ni, 7.58. $MnCl_2(NIT2\text{-}Py)_2{\cdot}2CH_2Cl_2$ (**2**): yield 27%; mp 197 °C. Anal. Calcd for $C_{26}H_{36}N_6O_4Cl_6Mn$: C, 40.84; H, 4.75; N, 11.00; O 8.38; Cl, 27.84; Mn, 7.19. Found: C, 40.98; H, 4.83; N, 10.79; Cl, 27.72; Mn, 7.26.

(b) Hexafluoroacetylacetonate Derivatives. (2-(2-Pyridyl-4,4,5,5-tetramethyl-4,5-dihydro-1*H*-imidazolyl-1-oxy 3-oxide)bis(hexafluoroacetylacetonato)nickel(II), $Ni(hfac)_2NIT2\text{-}Py$ (**3**), and (2-(2-pyridyl)-4,4,5,5-tetramethyl-4,5-dihydro-1*H*-imidazolyl-1-oxy 3-oxide)-bis(hexafluoroacetylacetonato)manganese(II), $Mn(hfac)_2NIT2\text{-}Py$ (**4**), were prepared by mixing 0.2 mmol of NIT2-Py and 0.2 mmol of the appropriate metal hexafluoroacetylacetonate in 5 mL of methylene chloride and 10 mL of heptane. Slow evaporation of these solutions at room temperature in the dark afforded the adducts. $Ni(hfac)_2NIT2\text{-}Py$: yield 56%; mp 137 °C. Anal. Calcd for $C_{22}H_{18}F_{12}N_3O_6Ni$: C, 37.35; H, 2.57; F, 32.25; N, 5.94; O, 13.58; Ni, 8.30. Found: C, 37.29; H, 2.75; F, 31.88; N, 5.84; Ni, 8.43. $Mn(hfac)_2NIT2\text{-}Py$: yield 36%; mp 151 °C. Anal. Calcd for $C_{22}H_{18}F_{12}N_3O_6Mn$: C, 37.55; H, 2.58; F, 32.43; N, 5.98; O, 13.65; Mn, 7.81. Found: C, 37.41; H, 2.45; F, 32.08; N, 5.84; Mn, 7.63.

(21) Funck, L. L.; Ortolano, T. R. *Inorg. Chem.* **1968**, *7*, 567–573.

Table I. Crystallographic Data

	1	**2**
chem formula	$C_{16}H_{36}NiCl_6N_6O_4$	$C_{26}H_{36}Cl_6MnN_6O_4$
fw	767.76	764.00
space group	$P2_1/c$ (No. 14)	$P2_1/c$ (No. 14)
a (Å)	8.890(2)	9.018(2)
b (Å)	13.957(2)	13.815(3)
c (Å)	13.802(2)	14.095(2)
β (deg)	103.06(2)	102.90(2)
V (Å^3)	1668.2	1711.6
Z	2	2
T (°C)	20	20
ρ(calcd) (g/cm^3)	1.527	1.489
μ/(cm^{-1})	1.1	1.1
R^a	0.042	0.061
$R_w{}^b$	0.038	0.057
	3	**5**
chem formula	$C_{22}H_{18}F_{12}N_3NiO_6$	$C_{22}H_{18}F_{12}MnN_3O_6$
fw	706.86	703.28
space group	$P2_1/c$ (No. 14)	$P2_1/c$ (No. 14)
a (Å)	11.866(2)	10.453(2)
b (Å)	14.173(2)	16.518(3)
c (Å)	17.282(3)	16.697(3)
β (deg)	95.66(1)	94.08(1)
V (Å^3)	2892.3	2875.6
Z	4	4
T (°C)	20	20
ρ(calcd) (g/cm^3)	1.623	1.625
μ (cm^{-1})	0.55	0.55
R^a	0.069	0.061
$R_w{}^b$	0.084	0.062

^{a} $R = \sum(F_o - F_c)/\sum wF_o$. ^{b} $R_w = (\sum w(F_o - F_c)^2/\sum wF_o^2)^{1/2}$.

EPR and Magnetic Measurements. Polycrystalline powder EPR spectra were recorded at X-band frequency with a Varian E9 spectrometer equipped with an Oxford Instrument ESR9 liquid-helium continuous-flow cryostat.

Magnetic data were collected in the 6-300 K temperature range using an SHE superconducting SQUID susceptometer or in the 2–300 K range using a Quantum Design MPMS susceptometer, both working at a 0.5-T field strength. The SQUID outputs were corrected for the magnetization of the sample holder, and the molar susceptibilites were corrected for the diamagnetism of the constituent atoms by using Pascal constants.

X-ray Data Collection. The above syntheses afforded, for all compounds **1–4**, crystals suitable by X-ray diffraction studies.

Preliminary Weissenberg photographs showed, for the four complexes, the same crystal system and space group: monoclinic, $P2_1/c$. Crystals of approximate dimensions 0.2 × 0.2 × 0.2 mm were mounted on an Enraf-Nonius CAD4 four-circle diffractometer equipped using graphite-monochromatized Mo Kα radiation. Accurate cell constants were derived from least-squares fitting of the setting angles of 25 independent reflections. They are reported in Table I. Data collections were performed at room temperature, checking periodically the intensities of three reflections. In all cases, no significant decrease of these intensities was noticed. The data were corrected for Lorentz and polarization factors but not for absorption.

Crystal Structure Determinations. (a) Metal Chloride Adducts. In both cases, the determination was straightforward: using direct methods (MULTAN[22]) and successive difference Fourier maps, the positions of the non-hydrogen atoms were determined. They were refined with anisotropic thermal parameters; in the last refinement model, hydrogen atoms were included at calculated and fixed positions with each thermal parameter equal to that of the connected atom.

(b) Hexafluoroacetylacetonate Derivatives. In these cases, the heavy-atom method was used (SHELX76 package[23]), and the positions of the metal ions, were determined from the Patterson maps. In the case of Mn(hfac)NIT2-Py (**4**), the positions of the other non-hydrogen atoms were obtained from difference Fourier maps. The refinement of the structure was carried out as described for the chloride adducts. Large

(22) Main, P.; Hull, S. E.; Lessinger, L.; Germain, G.; Declercq, J. P.; Woolfson, M. H. MULTAN 80. Universities of York, England, and Louvain, Belgium, 1980.

(23) Sheldrick, G. SHELX76 System of Computing Programs. University of Cambridge, England, 1976.

Table II. Positional Parameters (×10⁴) and B_{eq} Values for **1**

	x	y	z	B_{eq}[a] (Å²)
Ni	0(0)	0(0)	0(0)	2.00
Cl1	1802(0)	1077(0)	1003(0)	2.65
O1	149(1)	−872(1)	1225(1)	2.60
O2	1538(2)	−3779(1)	64(1)	4.06
N1	271(2)	−1784(1)	1078(1)	2.19
N2	926(2)	−3160(1)	531(1)	2.68
N3	1849(2)	−792(1)	−280(1)	2.15
C1	1132(2)	−2197(1)	515(1)	2.17
C2	−327(2)	−3430(1)	1053(1)	2.75
C3	−403(2)	−2506(1)	1668(1)	2.38
C4	124(3)	−4329(2)	1662(2)	4.18
C5	−1770(3)	−3599(2)	225(2)	4.04
C6	−2020(3)	−2198(1)	1739(2)	3.56
C7	674(3)	−2518(2)	2695(1)	3.42
C8	2189(2)	−1706(1)	8(1)	2.14
C9	3501(2)	−2175(1)	−135(1)	2.85
C10	4479(2)	−1695(2)	−615(2)	3.19
C11	4137(2)	−772(2)	−925(2)	3.15
C12	2826(2)	−346(1)	−743(1)	2.76
Cl2	5218(1)	355(0)	3613(0)	9.19
Cl3	4556(1)	−1399(0)	2508(0)	8.04
C13	3783(3)	−432(2)	3047(2)	6.01

[a] $B_{eq} = {}^4/_3\sum\beta_{ij}a_ia_j$.

Table III. Positional Parameters (×10⁴) and B_{eq} Values for **2**

	x	y	z	B_{eq}[a] (Å²)
Mn	0(0)	5000(0)	5000(0)	2.29
Cl1	−1838(1)	3872(0)	4015(0)	2.94
O1	−313(2)	5924(1)	3727(1)	3.01
O2	−1549(3)	8820(2)	4917(2)	5.07
N1	−379(3)	6829(2)	3892(2)	2.49
N2	−967(3)	8197(2)	4443(2)	3.04
N3	−1971(3)	5889(2)	5266(2)	2.34
C1	−1224(4)	7249(2)	4450(2)	2.43
C2	294(4)	8444(2)	3932(2)	2.94
C3	349(4)	7523(2)	3316(2)	2.63
C4	−132(5)	9338(2)	3309(3)	4.40
C5	1716(4)	8605(3)	4747(3)	4.33
C6	−686(4)	7552(3)	2284(2)	3.66
C7	1926(4)	7190(3)	3275(3)	3.91
C8	−2288(3)	6784(2)	4960(2)	2.33
C9	−3561(4)	7269(2)	5095(2)	3.14
C10	−4552(4)	6812(3)	5560(3)	3.70
C11	−4247(4)	5893(3)	5889(3)	3.58
C12	−2955(4)	5464(2)	5713(2)	2.97
Cl2	4572(1)	1375(1)	2453(1)	9.02
Cl3	5179(2)	−323(1)	3598(1)	10.44
C13	3760(5)	434(4)	2987(3)	6.42

[a] $B_{eq} = {}^4/_3\sum\beta_{ij}a_ia_j$.

thermal parameters were observed for the fluorine atoms, but examination of a difference Fourier map showed no peak higher than 0.5 e Å^{-3} and no depression lower than 0.35 e Å^{-3}.

In contrast, in Ni(hfac)$_2$NIT2-Py (**3**), two of the CF_3 groups were found to be disordered about the C–C bonds (C3–C5 and C6–C9) connecting them to the acetylacetonate ligand. The disorder was such that two separate sets of fluorine atoms could be seen in a difference Fourier map in each case. On the basis of the interpolated heights of the peaks for these partial atoms in the map, fixed population parameters of 0.5 were assigned for F4A, F5A, F6A and F4B, F5B, F6B. Corresponding parameters were 0.7 and 0.3 for atoms F7A–F9A and F7B–F9B, respectively. The final refinement model included these atoms with anisotropic thermal parameters and the hydrogen atoms with isotropic thermal parameters equal to those of the connected carbons. On the final cycle, no parameter shift for any non-fluorine atom as well as for the CF_3 groups which showed no disorder was greater than 35% of the standard deviation in that parameter. For the CF_3 groups modeled with partial occupancy, six parameters had shifts larger than one standard deviation. A final Fourier map showed no peak (positive or negative) higher than 0.90 e Å^{-3}.

For the four compounds, the final R values are reported in Table I with other experimental parameters. Atomic positional parameters are found in Tables II-V, and selected bond lengths and angles, in Table VI.

A summary of crystal data and experimental parameters (Table SI)

Table IV. Positional Parameters (×10⁴) and B_{eq} Values for **3**

	x	y	z	B_{eq}[a] (Å²)
Ni	3725(1)	2463(0)	550(0)	4.77
O1	4820(2)	3487(2)	288(2)	3.85
O2	8156(3)	1833(3)	234(3)	7.35
O3	2586(3)	2770(2)	−368(2)	4.22
O4	2677(3)	1443(2)	878(2)	4.22
O5	2898(3)	3407(2)	1166(2)	4.66
O6	4746(2)	2113(2)	1528(2)	4.00
N1	5874(3)	3256(2)	374(2)	3.46
N2	7457(3)	2481(3)	345(3)	4.82
N3	4601(3)	1581(2)	−136(2)	3.40
C1	6319(4)	2451(3)	164(3)	3.62
C2	6768(4)	3974(3)	642(4)	5.31
C3	7804(4)	3341(4)	828(4)	5.47
C4	6868(6)	4613(4)	−78(5)	7.83
C5	6396(6)	4556(6)	1274(6)	12.55
C6	7941(8)	2986(7)	1688(4)	9.75
C7	8925(5)	3695(5)	636(5)	7.47
C8	5701(3)	1677(3)	−241(2)	3.47
C9	6238(4)	1081(3)	−734(3)	4.52
C10	5627(5)	368(3)	−1125(3)	4.78
C11	4519(5)	273(3)	−1028(3)	4.50
C12	4014(4)	889(3)	−532(2)	3.82
C13	862(5)	2974(5)	−1112(3)	5.85
C14	1583(4)	2496(3)	−438(3)	4.11
C15	1052(4)	1855(3)	20(3)	4.66
C16	1627(4)	1394(3)	638(3)	4.11
C17	976(5)	720(4)	1133(3)	5.51
C18	2077(6)	4088(6)	2209(4)	6.79
C19	2942(4)	3402(3)	1898(3)	4.54
C20	3618(4)	2884(4)	2428(3)	4.81
C21	4470(4)	2284(3)	2200(3)	4.11
C22	5205(5)	1748(4)	2853(3)	4.99
F1	1410(4)	3083(5)	−1720(2)	11.39
F2	−87(4)	2579(4)	−1311(3)	11.27
F3	614(4)	3848(3)	−920(3)	9.98
F4a	1569(11)	139(12)	1501(12)	8.74
F5a	110(13)	332(13)	749(11)	10.13
F6a	486(14)	1220(10)	1632(9)	9.02
F7a	2099(9)	4039(9)	2981(5)	8.47
F8a	1048(6)	3803(10)	2000(4)	9.23
F9a	2296(12)	4948(5)	2022(10)	11.41
F7b	1534(23)	4660(24)	1633(12)	11.23
F8b	2341(30)	4526(30)	2800(29)	15.93
F9b	1410(38)	3847(27)	2597(67)	36.85
F4b	1224(27)	827(19)	1845(7)	14.97
F5b	1277(13)	−167(7)	1012(12)	9.81
F6b	−80(11)	691(14)	956(13)	10.43
F10	4812(4)	1789(3)	3527(2)	7.57
F11	6208(4)	2111(4)	2954(3)	9.78
F12	5274(4)	862(3)	2681(2)	8.70

[a] $B_{eq} = {}^4/_3\sum\beta_{ij}a_ia_j$.

and complete listings of bond lengths (Tables SII-SV), bond angles (Tables SVI-IX), and anisotropic thermal parameters (Tables SX-SXIII) are deposited as supplementary material.

Results

Structural Properties. (a) Metal Chloride Derivatives. As shown in Figure 2 for the Ni compounds, both complexes, **1** and **2**, are centrosymmetric tetragonally distorted octahedral species in which the apical sites are occupied by the chloride ions at 2.397(0) and 2.474(0) Å for the Ni and the Mn complex, respectively. The only noticeable distortions from this idealized bonding pattern are found in the O(nitroxide)–metal–N(pyridyl) angles (86.1(0)° for Ni and 80.4(0)° for Mn), which are significantly different from 90° because they are included in the chelate ring. Relevant structural parameters are listed in Table VII. In the two complexes, the radical moiety has almost the same conformation and the same coordination parameters, which are the consequence of the chelate ring structure. Small variations in the structural parameters for the organic ligand reflect the differences in the pyridyl nitrogen bonding lengths, which increase from nickel to manganese and release the strain of the ring. These

Table V. Positional Parameters (×10⁴) and B_{eq} Values for 4

	x	y	z	B_{eq}[a] (Å²)
Mn	2133(1)	2360(1)	4847(1)	3.92
O1	3753(4)	2298(3)	5710(2)	4.08
O2	3246(4)	3298(3)	4343(3)	3.49
O3	1025(4)	3096(3)	5590(3)	6.21
O4	625(4)	2656(3)	3952(2)	4.67
O5	1353(4)	1253(3)	5272(2)	5.82
O6	4213(4)	-767(3)	4688(3)	7.88
N1	2768(4)	1485(3)	3895(3)	4.15
N2	2047(4)	601(3)	5314(3)	3.74
N3	3361(5)	-374(3)	5032(3)	4.40
C1	4786(5)	2682(4)	5720(3)	3.68
C2	5154(6)	3268(4)	5190(4)	4.31
C3	4349(6)	3528(4)	4551(4)	4.41
C4	5727(7)	2496(6)	6446(4)	4.42
C5	4830(8)	4194(5)	4008(4)	5.41
C6	59(6)	3509(4)	5396(4)	5.19
C7	-614(6)	3574(4)	4645(4)	5.35
C8	-266(6)	3148(4)	3995(4)	3.91
C9	-424(10)	4007(7)	6080(6)	9.45
C10	-1011(9)	3258(6)	3189(6)	5.16
C11	2787(5)	334(4)	4768(4)	3.71
C12	2725(6)	-702(5)	5748(4)	5.96
C13	2125(6)	85(5)	6070(4)	4.56
C14	762(7)	-28(5)	6342(4)	9.52
C15	2997(9)	542(6)	6675(4)	4.45
C16	3704(7)	-1115(6)	6319(5)	11.43
C17	1729(7)	-1312(5)	5406(5)	6.98
C18	2891(5)	674(4)	3971(3)	3.43
C19	3040(6)	160(4)	3316(4)	4.62
C20	3036(7)	498(5)	2566(4)	5.79
C21	2922(6)	1322(5)	2475(4)	6.05
C22	2802(6)	1802(4)	3155(4)	5.53
F1	5430(5)	1884(4)	6855(3)	5.53
F2	6885(4)	2340(4)	6235(3)	8.74
F3	5879(6)	3126(4)	6903(3)	5.77
F4	5921(5)	4532(3)	4278(3)	6.65
F5	4002(6)	4800(3)	3909(3)	13.53
F6	4974(5)	3924(3)	3285(3)	10.69
F7	389(7)	4561(4)	6313(4)	9.95
F8	-471(9)	3597(5)	6733(5)	28.83
F9	-1470(7)	4350(6)	5945(5)	19.05
F10	-414(9)	3550(8)	2672(5)	13.19
F11	-1920(10)	3750(7)	3198(5)	17.50
F12	-1490(7)	2639(4)	2908(4)	-0.16

[a] $B_{eq} = {}^4/_3\sum\beta_{ij}a_ia_j$.

two new adducts are unambiguously elongated octahedral species with the oxygen (nitroxyl) atom equatorially bound. Interestingly, the N–O distance is 0.02 Å longer in the coordinated nitroxyl group than in the other one. The methylene chloride molecules of crystallization are arranged in layers, so that the three-spin species are well separated from each other.

(b) Hexafluoroacetylacetonate Derivatives. Examination of bond lengths and angles (Table VI) around the metal ion shows that these complexes also are distorted octahedral species (Figure 3). As observed in the metal chloride complexes, the metal–nitrogen bond is slightly longer than the metal–oxygen one, this difference being more pronounced for the manganese adduct, as expected. In both compounds, the structural features of the organic ligand (Table VII) are close to those observed in the complexes of the metal chlorides. In particular, the angle of the pyridyl ring with the mean plane of the radical is spread over a small angular range (28–35°). With the exception of the metal–O(nitroxyl) distance, which varies with the nature of the metal ion, the coordinations of the free radicals, as gauged by the angle between the M–O–N(nitroxide) plane and the radical plane, which is close to 45°, are very similar in all complexes. However, within the cell, important differences in crystal packing are observed. While the molecules are well shielded by the methylene chloride moieties in the chloride derivatives, in compounds 3 and 4, intermolecular contacts between NO groups belonging to molecules related by the inversion center are observed and may play a role in the solid-state magnetic behavior. In the manganese

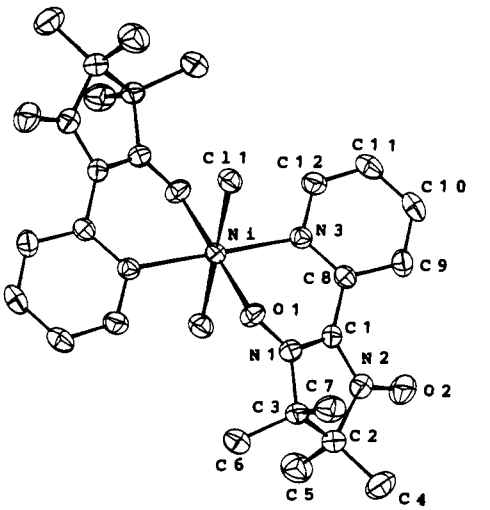

Figure 2. View of the molecular structure of 1 with thermal ellipsoids drawn at a 30% probability level. The numbering of the atoms applies to 2 as well.

Table VI. Selected Bond Lengths (Å) and Angles (deg)

		$NiCl_2(NIT2\text{-}Py)_2{\cdot}2CH_2Cl_2$ (1)			
Ni–Cl1	2.397(10)	Ni–N3	2.089(1)	Ni–O1	2.064(1)
O1–N1	1.297(2)	O2–N2	1.271(2)		
Cl1–Ni–O1	89.2(0)	Cl1–Ni–N3	89.3(0)	O1–Ni–N3	86.1(0)
Ni–O1–N1	116.3(1)	Ni–N3–C8	125.3(1)	Ni–N3–C12	117.6(1)
		$MnCl_2(NIT2\text{-}Py)_2{\cdot}2CH_2Cl_2$ (2)			
Mn–Cl1	2.474(0)	Mn–N3	2.271(2)	Mn–O1	2.155(2)
O1–N1	1.299(3)	O2–N2	1.276(3)		
Cl1–Mn–O1	89.4(0)	Cl1–Mn–N3	89.5(0)	O1–Mn–N3	80.4(0)
Mn–O1–N1	117.0(1)	Mn–N3–C8	126.0(2)	Mn–N3–C12	117.0(2)
		Ni(hfac)₂NIT2-Py (3)			
Ni–O1	2.029(3)	Ni–O2	2.024(3)	Ni–O3	2.023(3)
Ni–O4	2.041(3)	Ni–O5	2.029(2)	Ni–N1	2.073(3)
O5–N2	1.287(4)	O6–N3	1.265(5)		
O1–Ni–O4	174.6(1)	O2–Ni–O5	176.6(1)	O3–Ni–N1	175.6(1)
O1–Ni–O5	93.7(1)	O1–Ni–N1	90.8(1)	O2–Ni–N1	95.0(1)
O3–Ni–O5	89.9(1)	O4–Ni–O5	91.0(1)	O4–Ni–N1	92.1(1)
O5–Ni–N1	86.3(1)	Ni–O5–N2	115.4(2)	Ni–N1–C18	124.4(3)
Ni–N1–C22	117.8(3)				
		$Mn(hfac)_2NIT2\text{-}Py$ (4)			
Mn–O1	2.144(3)	Mn–O2	2.144(5)	Mn–O3	2.135(5)
Mn–O4	2.147(3)	Mn–O5	2.141(4)	Mn–N1	2.279(5)
O5–N2	1.297(6)	O6–N3	1.272(7)		
O1–Mn–O4	169.1(2)	O2–Mn–O5	167.3(2)	O3–Mn–N1	164.1(2)
O1–Mn–O5	92.3(2)	O1–Mn–N1	100.4(2)	O2–Mn–N1	89.5(2)
O3–Mn–O5	93.3(2)	O4–Mn–O5	98.3(2)	O4–Mn–N1	84.1(2)
O5–Mn–N1	80.1(2)	Mn–O5–N2	120.0(3)	Mn–N1–C18	126.4(4)
Mn–N1–C22	114.9(4)				

species, these contacts involve the uncoordinated NO groups, as observed in several metal–nitroxide derivatives where only one NO group is coordinated. On the other hand, in the nickel analogue, these "free" groups are far apart (>8 Å) and the closest contacts involve the coordinated NO groups of molecules deduced by the inversion center and an $a+b$ translation. However, in this case, the distances are larger (4.8 vs 3.4 Å) and it is expected that intermolecular magnetic interactions will be more active in the manganese compound than in the nickel complex.

Magnetic Properties. (a) Metal Chloride Derivatives. Magnetic data for 1 and 2 are reported in Figures 4and 5 in the form of χT vs T. The high-temperature values, χT = 1.362 emu K mol⁻¹ (μ = 3.30 μ_B) for 1 and χT = 3.01 emu K mol⁻¹ (μ = 4.91 μ_B) for 2, are much lower than those expected for noninteracting species, pointing to strongly antiferromagnetically coupled systems. Moreover, the low-temperature values also agree with this expectation since a singlet ground state is observed for 1 and a quartet state corresponding to a χT value of 1.84 emu K mol⁻¹ is observed for 2. As shown in the preceding section, in the solid

Table VII. Conformational Parameters of the NIT2-Py Metal Complexes

compd	d_{M-O}[a]	d_{M-N}[b]	d_{N-O}[c]	α[d]	β[e]	γ[f]
(a) Metal Chloride Derivatives						
$NiCl_2(NIT2\text{-}Py)_2$ (**1**)	2.064(1)	2.089(1)	1.297(2)	116.3(1)	41(1)	28(1)
			1.271(2)			
$MnCl_2(NIT2\text{-}Py)_2$ (**2**)	2.155(2)	2.271(2)	1.299(3)	117.0(1)	48(1)	30(1)
			1.276(3)			
(b) Hexafluoroacetylacetonate Derivatives						
$Ni(hfac)_2NIT2\text{-}Py$ (**3**)	2.029(3)	2.073(4)	1.287(4)	115.4(5)	43(1)	27(1)
			1.265(6)			
$Mn(hfac)_2NIT2\text{-}Py$ (**4**)	2.141(4)	2.279(5)	1.297(6)	120.0(3)	42(1)	35(1)
			1.272(7)			

[a] Metal–O(nitroxide) distance (Å). [b] Metal–N(pyridyl) distance (Å). [c] N–O bond length for the coordinated group (up) and the uncoordinated group (down) (Å). [d] Metal–O–N(nitroxide) angle (deg). [e] Angle between the M–O–N plane and the nitroxide mean plane (deg). [f] Angle between the pyridyl plane and the nitroxide mean plane (deg).

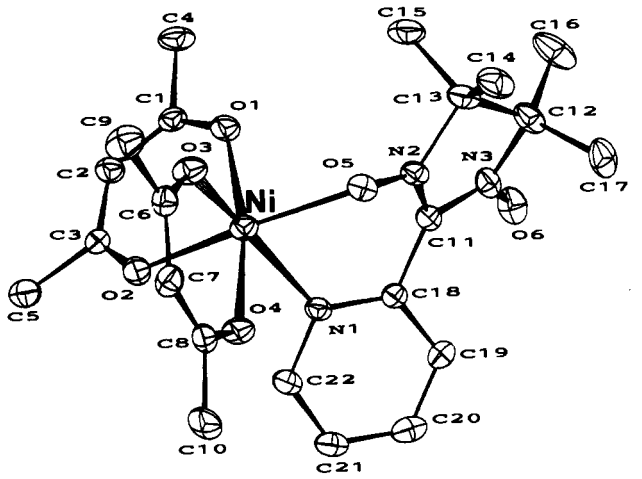

Figure 3. View of the molecular structure of **3** with thermal ellipsoids drawn at a 30% probability level. The fluorine atoms have been omitted for the sake of clarity. The numbering of the atoms applies to **4** as well.

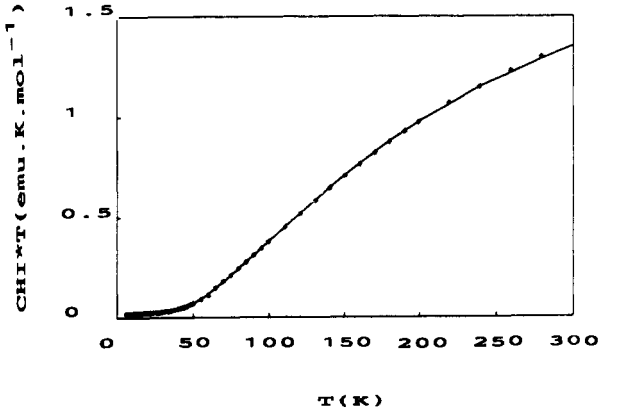

Figure 4. Temperature dependence of the magnetic susceptibilities for **1** in the form of χT vs T. The solid line was calculated with the parameters reported in Table VIIIa.

state, these complexes may be considered as isolated three-spin systems. Accordingly, the corresponding magnetic data were interpreted using published analytical expressions for the magnetic susceptibility of such systems.[24] The results of the best fit are reported in Table VIIIa.

(b) Hexafluoroacetylacetonate Derivatives. The temperature dependence of the χT products shown in Figures 6 and 7 for **3** and **4**, respectively, also point to antiferromagnetically coupled species. Indeed, the 300 K values (0.87 and 3.46 emu K mol^{-1} for **3** and **4**, respectively) are weaker than those expected for uncorrelated spins. Moreover, upon a decrease in the temperature, the χT product decreases. However, low-temperature behaviors are strikingly different in the two complexes: while a finite nonzero value of χT (0.476 emu K mol^{-1}) corresponding to a doublet state is reached for the Ni adduct, the sharp decrease observed for the Mn complex points to a singlet ground state. In the latter case, the structural results afford a reasonable dimer mode for interpreting the magnetic data. Assuming a four-spin system,[25] one obtains the set of parameters listed in Table VIIIb, which shows a fairly large intramolecular Mn(II)–nitroxide antifer-

(24) Sinn, E. *Coord. Chem. Rev.* **1970**, *5*, 313–347.

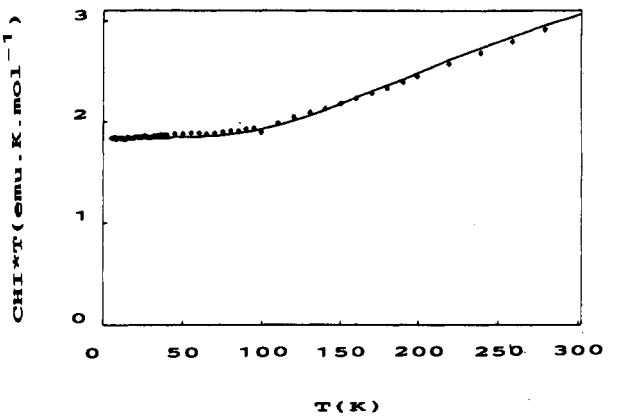

Figure 5. Temperature dependence of the magnetic susceptibilities for **2** in the form of χT vs T. The solid line was calculated with the parameters reported in Table VIIIa.

Table VIII. Summary of the Magnetic Parameters

compd	g	10^6TIP	J_1[a] (cm^{-1})	J_2[a] (cm^{-1})	10^4R[b]
(a) Metal Chloride Derivatives					
$NiCl_2(NIT2\text{-}Py)_2$ (**1**)	2.267(12)	182(11)	−110(11)		3.7
$MnCl_2(NIT2\text{-}Py)_2$ (**2**)	1.998(5)	74(7)	−79(5)		0.2
(b) Hexafluoroacetylacetonate Derivatives					
$Ni(hfac)_2NIT2\text{-}Py$ (**3**)	2.268(16)	161(6)	−167(6)	0	0.6
$Mn(hfac)_2NIT2\text{-}Py$ (**4**)	1.997(4)	66(8)	−65(2)	−36(1)	1.6

[a] The Hamiltonian used was in the form $H = -2JS_iS_j$. [b] The function minimized in the fitting process was $R = \sum(\chi_{obsd} - \chi_{calcd})^2/\sum(\chi_{obsd})^2$.

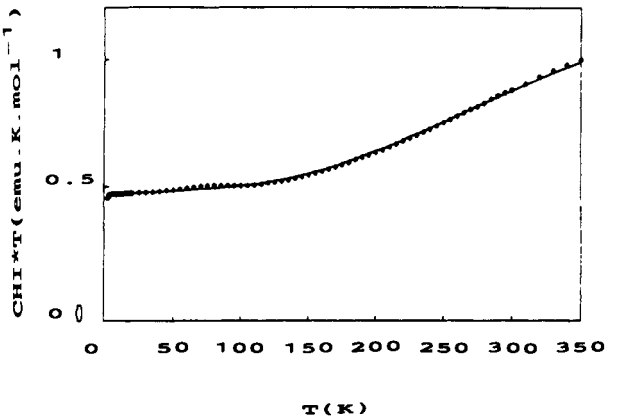

Figure 6. Temperature dependence of the magnetic susceptibilities for **2** in the form of χT vs T. The solid line was calculated with the parameters reported in Table VIIIb.

(25) Belorizky, E.; Friess, P. H.; Gojon, E.; Latour, J. M. *Mol. Phys.* **1987**, *61*, 661–666.

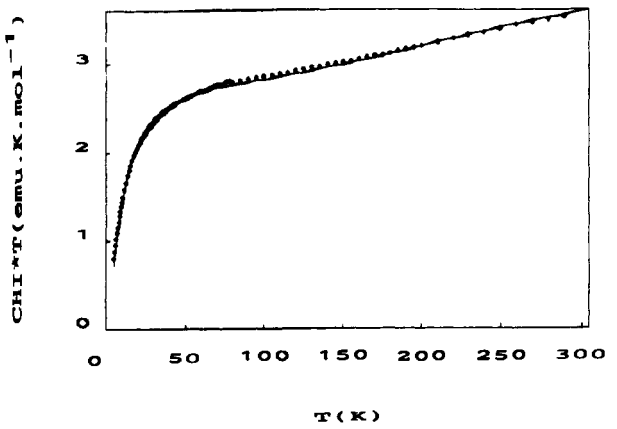

Figure 7. Temperature dependence of the magnetic susceptibilities for **4** in the form of χT vs T. The solid line was calculated with the parameters reported in Table VIIIb.

romagnetic coupling (J_1 = –65(2) cm^{-1}) and a moderate intermolecular (nitroxide–nitroxide) interaction J_2 = –36(1) cm^{-1}. Since in the Ni derivative a dimer model is also suggested by the structural results, we collected the magnetic data down to the lowest temperature we could reach (2 K) in order to check if some intermolecular coupling were operative below 5 K. A constant value of χT is observed at low temperature, so that we fitted the magnetic data to a two-spin model. The best fit affords a large Ni(II)–nitroxide antiferromagnetic coupling of J_1 = –167(6) cm^{-1} (Table VIIIb).

Finally, EPR spectra of polycrystalline samples are in good agreement with the magnetic data for the four complexes. Thus, for **1** at 300 K only a weak and broad signal is observed around g = 2 which vanishes at low temperature. In contrast, for **2** at 4.2 K, broad features at g = 3.32, 2.06, and 1.23 are compatible with an $S = {}^3/_2$ ground state. Both hfac derivatives exhibit a broad line (600 Oe) centered at g = 2 at room temperature. At 10 K, however, the spectrum of the nickel derivative is characteristic of a Kramer doublet, and assuming a g value of 2 for the nitroxide, g_{Ni} = 2.17 and g_{Ni} = 2.20 are obtained, which are reasonable values for an octahedral Ni(II) ion. Concerning **4**, at low temperature only a weak half-field transition appears; understanding of these features would require a complete analysis using single crystals.

Discussion

The main result of this study is the obtention, for the first time, of adducts of a nitroxide ligand with $NiCl_2$ and $MnCl_2$ in which the nitroxyl group is coordinated. This result shows that the chelate effect is a significant driving force for the coordination of nitroxyl groups to poor electrophilic metal centers.

Worth noting is the obtention of discrete species, whatever the stoichiometry of the starting reactants. We attempted to react the metal chloride derivatives with the homologous metal hexafluoroacetylacetonates, expecting the formation of extended adducts owing to the binding of the uncoordinated NO group to the acidic metal ion. In both cases, the only characterized compounds were **3** and **4** resulting from displacement of the radical ligand from the chloride adduct. These M(hfac)$_2$NIT2-Py complexes also are discrete adducts, probably because the pyridyl group has too many steric requirements, as observed for the closely related phenyl analogue.[1,6]

Since Doedens's work describing the first structurally characterized adducts of Ni(II) and Mn(II) with Tempo and Proxyl nitroxides[26,27] (Figure 1), several nitronyl nitroxide complexes of these metal ions have been reported.[13-15,19,28,29] Qualitatively, they all are antiferromagnetically coupled species; the magnitude of the interactions arising from direct ligation of the nitroxyl oxygen atom has been rationalized in the frame of extended Huckel calculations.[28] Compared to the previously reported examples, understanding of the magnetic data for **1**–**4** must take into account a new contribution: the indirect coupling through a possible delocalization of the spin density onto the pyridyl imino atom providing a second exchange pathway. This contribution is difficult to figure out since even sophisticated theoretical calculations hardly give correct estimates of coupling constants.[30] However, a recent polarized neutron diffraction study shows that in NITPh (Figure 1) less than 1% of the spin density is delocalized on each carbon atom of the phenyl ring.[31] Since, in the solid state, NITPh has a twisted conformation[32] similar to that observed for NIT2-Py in **1**–**4** (30–40°), these neutron data may be use as a crude estimate of the delocalization of the spin density on the pyridyl group. Therefore, in first approximation, the contribution of the new pathway induced by the formation of the chelate ring may be neglected.

Manganese Derivatives. Axial ligation of nitroxides to manganese seems to be the rule, and most of the known adducts are trans-diaxial antiferromagnetically coupled species.[26-28] Only a few cis derivatives involving equatorially bound radical ligands have been reported for the less hindered nitroxide, NITMe,[28] or in chain compounds where interactions such as the coordination of the second NO group stabilizes a cis arrangement of two radicals.[14] However, in these cis bis(radical) adducts, it was not possible to distinguish two coupling constants, so that the exchange interaction between a Mn(II) ion and an equatorially bound nitroxide is not accurately known. Both compounds **2** and **4** are equatorial species which afford the proper structural features to proxide insight into the understanding of the coupling mechanism in these metal complexes.

Manganese–nitroxide magnetic interactions are spread over a 200-cm^{-1} energy range. Owing to the five metal magnetic orbitals, correlation between structure and coupling magnitude has only been attempted.[28] Axial complexes exhibit Mn–O(nitroxyl) bond lengths in the range 2.127(5)–2.177(8) Å while the equatorial binding distances are slightly shorter (2.101(10)–2.122(5) Å). The corresponding values observed for **2** and **4** (2.155(2) and 2.141(4) Å) are slightly larger than expected as a probable consequence of the strain in the chelate ring. Keeping in mind that antiferromagnetic couplings are related to the overlap of magnetic orbitals,[33] this larger binding distance associated to the M–O–N(nitroxide) angle is of importance. This angle is close to 130° in both axial and equatorial complexes except in Mn(hfac)$_2$(Tempo)$_2$ (167.2(3)°) and in our two adducts (117.0(1) and 120.0(3) for **2** and **4**, respectively). Assuming that the magnitude of the interaction arises primarily from overlap of the nitroxide π^* orbital and the metal orbital pointing toward the ligand, the wide angle in Mn(hfac)$_2$(Tempo)$_2$ does not favor a large interaction (–79 cm^{-1}).[27] On the other hand, a smaller angle in **2** and **4** suggests a larger metal–radical interaction. Actually, our compounds exhibit the weakest intramolecular interactions reported so far for manganese–nitroxide complexes. While in all reported Mn(II)–nitroxide adducts the Mn–O–N(nitroxide) plane is roughly perpendicular to the radical mean plane, this angle is only about 45° in the two studied complexes. The latter parameter, in reducing significantly the overlap between

(26) Porter, L. C.; Dickman, M. H.; Doedens, R. J. *Inorg. Chem.* **1988**, *27*, 1548–1552.
(27) Dickman, M. H.; Porter, L. C.; Doedens, R. J. *Inorg. Chem.* **1986**, *25*, 2595–2599.
(28) Caneschi, A.; Gatteschi, D.; Laugier, J.; Pardi, L.; Rey, P.; Zanchini, C. *Inorg. Chem.* **1988**, *27*, 2027–2032.
(29) Benelli, C.; Caneschi, A.; Gatteschi, D.; Melandri, M. C.; Rey, P. *Inorg. Chim. Acta* **1990**, *172*, 137–141.
(30) Charlot, M. F.; Verdaguer, M.; Journaux, Y.; de Loth, P.; Daudey, J. P. *Inorg. Chem.* **1984**, *23*, 3802–3808.
(31) Ressouche, E.; Rey, P.; Schweizer, J.; Zheludev, A. To be published.
(32) Wong, W.; Watkins, S. F. *J. Chem. Soc., Chem. Commun.* **1973**, 888–889.
(33) Kahn, O. *Angew. Chem., Int. Ed. Engl.* **1985**, *24*, 834–850.

the magnetic orbitals, is probably the main cause of the weakness of the interactions in **2** and **4**. However, these interactions are sufficiently strong to be reflected in the bond length of the coordinated NO group, which is 0.02 Å longer than that of the uncoordinated one.

Finally, a rather strong intermolecular interaction (−36(1) cm^{-1}) is observed in **4**. Such couplings between uncoordinated NO groups have been previously described. The structural parameters of the centrosymmetric dimer structure in **4** are unexceptional and are in line with the magnitude of the observed interaction.

Nickel Derivatives. Only a few nickel–nitroxide complexes have been described;[20,26] they all exhibit large antiferromagnetic interactions. In comparison to the studies on manganese adducts, only two structural determinations of nickel–nitroxide complexes are available.[15,20] Even in these cases, a detailed analysis of the magnetic data was not performed because the range of temperature where the magnetic susceptibility was different from zero was rather narrow. Therefore, only lower limits of the nickel–nitroxide interactions have been reported (−200 cm^{-1}). The two complexes **1** and **3** are less coupled (−110(11) and −167(6) cm^{-1}) than the previously reported examples, so that the magnetic data could be precisely analyzed because the room-temperature values of χT were rather high (>1 emu K mol^{-1}), especially in the case of **3**, for which magnetic data were collected up to 350 K.

As for the manganese adducts and for the same reasons, it is seen that the formation of the chelate ring has strong influence on the magnetic coupling. Assuming that the pyridyl nitrogen binding is not important, it is the modification of the orientation of the magnetic orbitals due to ring formation which lessens the magnitude of the interaction.

Conclusion

This chelating ligand affords the expected metal–O(nitroxide)-bonded complexes with poor electrophilic metal centers. In these species, the formation of a chelate ring induces a weakening of the intramolecular metal–nitroxide interaction. From the synthetic point of view, only discrete species were obtained as a probable consequence of the pyridyl steric requirement; it is anticipated however, that an aminomethyl-substituted ligand could allow the synthesis of extended species possessing interesting magnetic properties.

Supplementary Material Available: Table SI (crystallographic data and experimental parameters), Tables SII–SV (bond lengths), Tables SVI–IX (bond angles), and Tables SX–SXIII (anisotropic thermal parameters) (18 pages). Ordering information is given on any current masthead page.